Наносистеми, наноматеріали, нанотехнології
Nanosistemi, Nanomateriali, Nanotehnologii
2025, т. 23, № 3, сс. 759–777
https://doi.org/10.15407/nnn.23.03.0759

PACS numbers: 52.80.Mg, 52.80.Tn, 52.90.+z, 79.60.Jv, 81.15.Gh, 81.16.-c, 82.33.Xj

Characteristics of the Pulse-Periodic Gas-Generating Source of Flows of Ultraviolet Radiation and Silver Sulphide Microstructures

O. K. Shuaibov, R. V. Hrytsak, O. Yo. Minya, A. O. Malinina,
O. M. Malinin, M. O. Marhitych, O. V. Zubaka, and M. M. Feldii

Uzhhorod National University,
3, Narodna Str.,
UA-88000 Uzhhorod, Ukraine

The research results on the synthesis conditions of surface microstructures of silver sulphide from the plasma of an overvoltage nanosecond discharge (OND) between electrodes made of polycrystalline Ag_2S compound in helium are presented. The discharge is ignited in atmospheric-pressure helium with a 2 mm-gap between the electrodes. Silver sulphide vapours are introduced into the He–Ag_2S gas–vapour mixture by means of the ectonic mechanism. The voltage pulses, current, pulsed discharge power, and energy input into the plasma per pulse are studied at pulse repetition frequencies of 40–1000 Hz. Spectral and spatial characteristics of the OND are analysed. Using micro-Raman spectroscopy of laser-radiation scattering, the Raman scattering spectra of thin films deposited from the OND plasma onto a quartz substrate located near the electrode system are investigated and analysed. Based on solving the stationary Boltzmann kinetic equation for the electron-energy distribution function, numerical modelling is performed for the plasma transport parameters, specific energy losses, and rate constants of electron processes as functions of the parameter E/N, where E is the electric-field strength, and N is the total particle concentration in the working mixture. The discharge can be utilized as a source of bactericidal radiation, a source of silver sulphide microstructures, and as a plasma-chemical reactor for synthesizing corresponding thin films.

Наведено результати дослідження умов синтези поверхневих мікроструктур сульфіду Арґентуму з плазми перенапруженого наносекундного розряду (ПНР) між електродами з полікристалічної сполуки Ag_2S в гелії. Розряд запалювався в гелії атмосферного тиску за віддалі між електродами у 2 мм. Пари сульфіду Арґентуму вносилися в газопарову суміш He–Ag_2S за рахунок ектонного механізму. Досліджено імпульси напруги, струму, імпульсна потужність розряду, енергетичний внесок у

плазму за один імпульс за частот повторення імпульсів у 40–1000 Гц. Досліджено спектральні та просторові характеристики ПНР. Методом мікрораманівської спектроскопії розсіяння лазерного випромінення досліджено та проаналізовано спектри Раманового розсіяння тонких плівок, які були осаджені з плазми ПНР на кварцову підкладинку, встановлену біля системи електрод. На основі рішення стаціонарного Больцманнова кінетичного рівняння для функції розподілу електронів за енергіями виконано числове моделювання транспортних параметрів плазми, питомих втрат енергії та констант швидкости електронних процесів в залежності від величини параметра E/N, де E — напруженість електричного поля, N — повна концентрація частинок у робочій суміші. Розряд може бути використаний як джерело бактерицидного випромінення та джерело мікроструктур сульфіду Арґентуму, а також як плазмохемічний реактор синтези відповідних тонких плівок.

Key words: overvoltage nanosecond discharge, silver sulphide, helium, radiation spectrum, Raman spectrum, thin film.

Ключові слова: перенапружений наносекундний розряд, сульфід Арґентуму, гелій, спектер випромінення, Раманів спектер, тонка плівка.

(Received 19 December, 2024)

1. INTRODUCTION

An overvoltage nanosecond discharge (OND) of atmospheric pressure between electrodes made of transition metals (Cu, Zn, Fe, Al) and the $CuInSe_2$ compound in air and oxygen was successfully used for the synthesis of surface micro-nanostructures of electrode material on a solid substrate installed near the electrode system [1–4]. The introduction of vapours of the electrode material in these cases occurred due to microexplosions of natural inhomogeneities of the electrode surface in the form of nanopoints in a strong electric field (formation of ectons) [5]. The plasma of such a discharge was quite homogeneous in space even without prior ionization of the interelectrode gap [6] and was a source ultraviolet radiation, therefore, the synthesis of these structural elements took place with the automatic assistance of ultraviolet radiation, which can be promising for improving the characteristics of the synthesized structures, conditions of application of such films in solar batteries and other optoelectronic devices.

A windowless OND-based reactor in atmospheric pressure air between transition metal electrodes was effectively a source of UV radiation streams and metal oxide nanoparticle streams that were automatically time-synchronized.

Therefore, it may be promising to use OND in inert gases at atmospheric pressure and for the synthesis of surface structures

based on superionic conductors such as Ag_2S, Ag_8GeS_6, *etc*. Such compounds are synthesized by various chemical methods initially in the form of macroscopic polycrystalline elements. However, their use in micro-nanotechnology requires the synthesis of such compounds in the form of thin films.

Physical methods for the synthesis of thin films based on superionic conductors were used in Ref. [8], where the synthesis of thin films from the Ag_2S compound in a magnetron discharge was reported, and the results of the synthesis of films from the Ag_2S compound, which was excited in the form of a vapour by a low-voltage electron beam ($E = 800–1600$ eV) are given in Ref. [9].

To optimize the process of gas-discharge synthesis of films of superionic conductors, it is necessary to study the characteristics and parameters of the OND plasma in inert gases between electrodes made of superionic conductors in the form of polycrystalline samples. Such characteristics and parameters of plasma currently do not exist. This restrains the development of new supercapacitors, batteries, photovoltaic devices and sensitive gas sensors based on superionic conductors.

The goal and task of this research is the development of new gas-discharge UV lamps based on the destruction products of superionic conductors (Ag_2S) and the development of a technique for the synthesis of thin nanostructured films with the properties of superionic conductors by using microexplosions of inhomogeneities on the surface of metal electrodes and electrodes made of superionic conductors in an overvoltage nanosecond electric field discharge (formation of ectons, flow of nanoparticles and clusters of electrode material and UV plasma radiation).

The article presents the results of an experimental study of electrical and optical characteristics and numerical modelling of the OND plasma parameters in helium at atmospheric pressure between silver sulphide electrodes. Thin films from the products of destruction of electrodes in plasma were synthesized and their qualitative composition was determined.

2. EXPERIMENTAL METHODOLOGY

Experimental measurements were carried out using the method of measuring the spectral analysis of the emission of light sources.

A bipolar high-voltage discharge with duration of 100–450 ns was ignited between two electrodes, which were made of a polycrystalline Ag_2S compound. The distance between the electrodes was 2 mm. The radius of rounding of the end parts of the cylindrical electrodes is of 10 mm. The diameter of the electrodes is of 5 mm.

Silver sulphide is a superionic conductor, and thin films based on

it are promising for use in high-voltage pulse technology (supercapacitors, *etc.*). Since such films contain silver, in addition to high ionic conductivity, they can also have bactericidal properties.

The scheme of the installation, the structure of the discharge device and other conditions for studying the characteristics of the OND are given in the work [4].

The discharge was ignited by overvoltage of the discharge gap, when a beam of runaway electrons is formed in it [6]. Under the action of such a beam, the discharge in atmospheric pressure helium was uniform and had an aperture close to square, the area of which was of 4 mm^2. In a strong electric field on the working surface of the electrode based on the Ag_2S superionic conductor, microexplosions of inhomogeneities occur on the surface of the electrodes [5], which contributed to the introduction of vapours of the superionic conductor Ag_2S products and their decay (Ag, Ag^+, S, ...) into the plasma and the formation of a flow of clusters and of nanoparticles based on the Ag_2S compound and its dissociation products in the plasma, which were further deposited on the quartz substrate in the form of thin films. For the synthesis of nanostructures of superionic conductors, which are intended for various applications in micro-nanotechnology, mainly chemical methods are used, *i.e.*, methods of exploding thin wires or plates, when a current pulse of hundreds to thousands of amperes passes through them. Therefore, the application of synthesis technologies of these nanostructures based on more technological and less expensive gas discharge technologies is promising. At the same time, it becomes possible to carry out the synthesis of nanostructures without the use of vacuum technology in low-cost gases, both in gasostatic conditions and in low-velocity gas flows.

The UV-radiation power density of the discharge was measured using a TKA-PCM UV meter at a distance of 15 cm from the centre of the discharge.

The surface of synthesized samples of thin films was examined with the help of a microscope with a magnification of 50 times.

The polycrystalline compound of silver sulphide (Ag_2S), from which the electrodes are made, was synthesized in the technological laboratory of the Uzhhorod National University.

The study of thin films of Ag_2S in helium at atmospheric pressure was carried out under the following conditions: the voltage at the anode of the thyratron modulator of high-voltage nanosecond pulses was of 13 kV, the frequency of following voltage pulses was of 80 Hz, the distance from the centre of the discharge to the glass plate was of 10 mm, the sputtering time was of five cycles of 30 minutes each. Analysis of thin films was carried out using three available laser wavelengths, 532, 633 and 785 nm, on a Renishaw

InVia confocal Raman microscope spectrometer at their 100% power of 60.6, 9.2 and 32 mW, respectively. The diameter of the laser beam was of 1–2 μm. The micro-Raman method is recognized as a powerful and versatile tool for the analysis of solid films and condensed media in general. This method is non-contact, which allows non-destructive and quantitative microanalysis of structural and electrical properties.

The OND plasma parameters were determined numerically and calculated as total integrals of the electron distribution function (EEDF). The EEDF was found by solving the Boltzmann kinetic equation in the binomial approximation [13]. EEDF calculations were carried out using the program [14]. Based on the obtained EEDF, the plasma parameters were calculated depending on the magnitude of the reduced electric field—E/N (the ratio of the electric field strength (E) to the total concentration of helium atoms and a small admixture of silver sulphide vapours (N)). The range of changes in the parameter $E/N = 1–1000$ Td ($1 \cdot 10^{-17}–1 \cdot 10^{-14}$ V·cm^2) included the values of the parameter E/N, which were implemented in the experiment. These values of the E/N parameter were of 327 Td and 53 Td at 0 ns and 180 ns from the start of the discharge, respectively (Fig. 1, *a*).

In the integral of collisions of electrons with helium atoms and silver atoms, the following processes are taken into account: elastic scattering of electrons on helium and silver atoms; excitation of the energy level of helium atoms (threshold energy of 19.80 eV); ionization of a helium atom (threshold energy of 24.58 eV); excitation of energy levels of atoms and silver ions (threshold energies of 6.01 eV, 5.99 eV, 3.78 eV, 3.66 eV, 7.19 eV, 7.02 eV, 6.71 eV, 5.99 eV, and 17.00 eV); ionization of silver atoms (threshold energy of 8.00 eV); electron–electron and electron–ion collisions. Effective sections of processes were taken from databases [15–18].

3. RESULTS AND DISCUSSION

In Figure 1, the oscillograms of voltage and current pulses, the pulsed power of the OND and the energy contribution to the plasma of the He–Ag_2S gas–vapour mixture for one discharge pulse are shown.

The total duration of voltage pulses reached 450 ns. The voltage pulse included oscillations decaying in time with duration of 40–50 ns. The maximum values of the electrical characteristics of the OND were observed at the atmospheric pressure of helium. Thus, the greatest drop in the value of the voltage of positive polarity during the discharge interval was of 17 kV, and the maximum amplitude of the pulse of the current of positive polarity reached 150 A. The maximum impulse power of the discharge was observed at

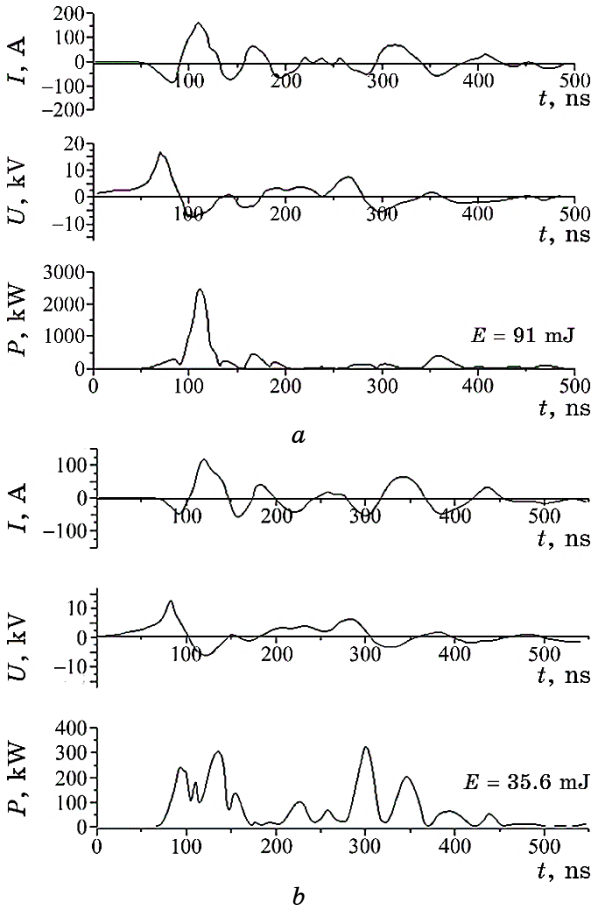

Fig. 1. Oscillograms of current pulses, voltages, pulsed power, and energy contribution to the plasma of an overvoltage nanosecond discharge for one discharge pulse: (*a*) p(He) = 101 kPa, (*b*) p(He) = 13.3 kPa; f = 1000 Hz.

p(He) = 101 kPa in the first 110 ns from the moment of its ignition and reached 2.3 MW (at t = 110 ns). The energy of a single electric pulse at p(He) = 101 kPa was of 91 mJ, and at p(He) = 13.3 kPa, it decreased to 35.6 mJ.

Let us consider the dependence of the radiation intensity of the discharge in He–Ag_2S gas–vapour mixtures on the value of the helium pressure and the main parameters of its excitation system—the pulse tracking frequency and the value of the charging voltage of the working capacitor of the high-voltage modulator of nanosecond pulses.

Figures 2, 3 present the dependence of the intensity of UV-radiation on the frequency of repetition of voltage pulses and the

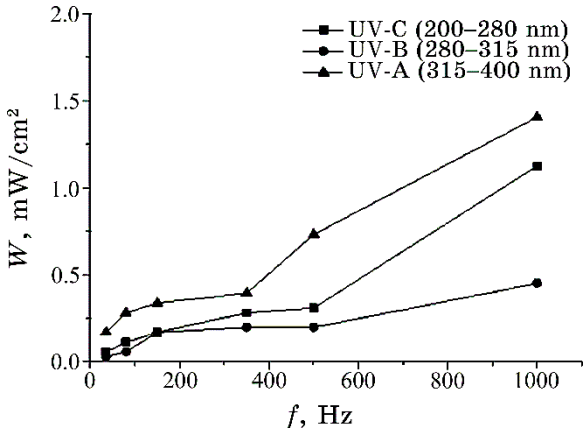

Fig. 2. Dependences of the UV-radiation intensity in the UV-C, UV-B, and UV-A ranges for OND plasma on the value of the repetition frequency of voltage pulses at a charging voltage of $U = 13$ kV in helium between Ag_2S electrodes at a He pressure of 101 kPa.

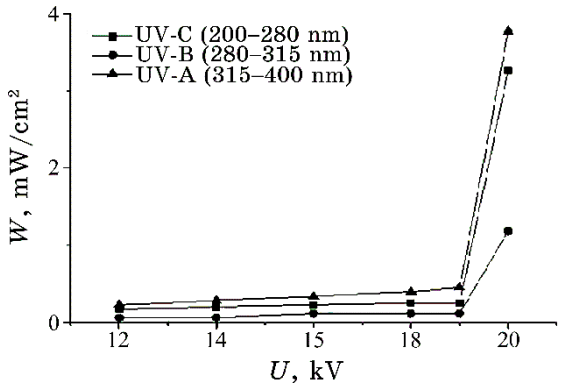

Fig. 3. Dependences of the UV-radiation intensity in the UV-C, UV-B, UV-A ranges for the OND plasma on the voltage on the electrodes at a frequency $f = 80$ Hz in helium between the Ag_2S electrodes at a He pressure of 101 kPa.

value of the charging voltage.

The highest value of the average power of plasma UV radiation was observed at a helium pressure equal to 101 kPa at a maximum frequency $f = 1000$ Hz and a charging voltage of 19 kV (Figs. 2, 3).

The emission spectra of OND in the He–Ag_2S gas–vapour mixture at different helium pressures and different repetition frequencies of voltage pulses are shown in Fig. 4. For the spectrum in Fig. 4, the reference book [10] was used to decode the spectrum.

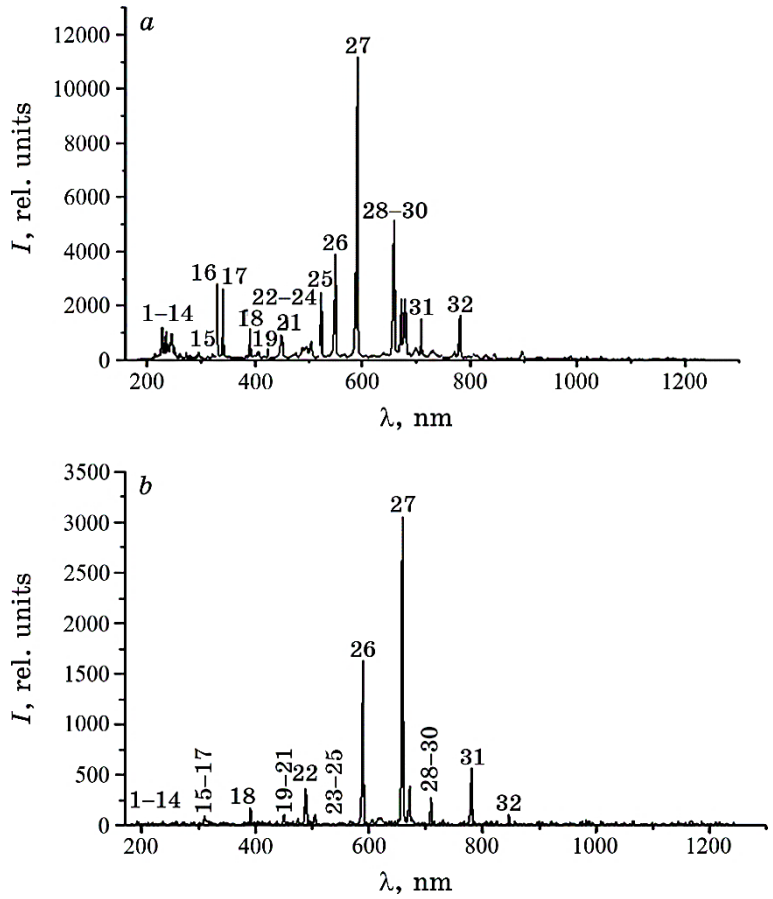

Fig. 4. The emission spectra of OND between the Ag_2S-compound electrodes at: p(He) = 101 kPa, f = 1000 Hz (*a*); p(He) = 13.3 kPa, f = 80 Hz (*b*).

TABLE 1. The maximum values of the power of UV-OND radiation in helium–silver sulphide steam–gas mixtures at different pressures of helium (U_{ch} = 20 kV, f = 1000 Hz).

Spectral range	p(He) = 13.3 kPa	p(He) = 101 kPa
	W, a.u.	W, a.u.
UV-C (200–280 nm)	1.4	3.3
UV-B (280–315 nm)	0.8	1.2
UV-A (315–400 nm)	1.7	3.8

As can be seen in Table 1, in the ultraviolet part of the OND-plasma spectrum, radiation at the transitions of an atom and a singly charged silver ion is prevailing.

The results of identification of spectral lines are shown in Table 2.

TABLE 2. The results of the identification of the emission spectra of OND between the electrodes of the Ag_2S compound at atmospheric pressure of helium (f = 1000 Hz).

No.	λ_{tab}, nm	I, a.u.	Object	E_{low}, eV	E_{upper}, eV	Lower$_{term}$	Upper$_{term}$
1	211.38	250	Ag*II*	4.85	10.71	$4d^9(^2D_{5/2})5s\ ^2[^5/_2]_3$	$4d^9(^2D_{5/2})5p\ ^2[^5/_2]_3$
2	224.64	1226	Ag*II*	4.85	10.37	$4d^9(^2D_{5/2})5s\ ^2[^5/_2]_3$	$4d^9(^2D_{5/2})5p\ ^2[^7/_2]_4$
3	227.99	582	Ag*II*	5.70	11.05	$4d^9(^2D_{3/2})5s\ ^2[^3/_2]_2$	$4d^9(^2D_{3/2})5p\ ^2[^5/_2]_3$
4	232.02	1514	Ag*II*	5.05	10.36	$4d^9(^2D_{5/2})\ 5s^2[^5/_2]_2$	$4d^9(^2D_{5/2})5p\ ^2[^3/_2]_1$
5	238.62	584	Ag*II*	11.14	16.34	$4d^9(^2D_{3/2})5p\ ^2[3/2]_1$	$4d^9(^2D_{3/2})5d\ ^2[3/2]_2$
6	241.13	975	Ag*II*	5.42	10.56	$4d^9(^2D_{3/2})5s\ ^2[3/2]_1$	$4d^9(^2D_{5/2})5p\ ^2[5/2]_2$
7	243.77	952	Ag*II*	4.85	9.94	$4d^9(^2D_{5/2})5s\ ^2[^5/_2]_3$	$4d^9(^2D_{5/2})5p\ ^2[^3/_2]_2$
8	244.78	580	Ag*II*	5.70	10.77	$4d^9(^2D_{3/2})5s\ ^2[3/2]_2$	$4d^9(^2D_{3/2})5p\ ^2[5/2]_2$
9	260.59	251	Ag*II*	10.18	14.94	$4d^9(^2D_{5/2})5p\ ^2[^7/_2]_3$	$4d^9(^2D_{5/2})6s\ ^2[^5/_2]_3$
12	271.17	254	Ag*II*	10.37	14.94	$4d^9(^2D_{5/2})5p\ ^2[^7/_2]_4$	$4d^9(^2D_{5/2})6s\ 2[^5/_2]_3$
13	276.75	150	Ag*II*	5.70	10.18	$4d^9(^2D_{3/2})5s\ ^2[3/2]_2$	$4d^9(^2D_{5/2})5p\ ^2[7/2]_3$
14	293.83	280	Ag*II*	10.77	14.99	$4d^9(^2D_{3/2})5p\ ^2[5/2]_2$	$4d_9(^2D_{5/2})6s\ ^2[5/2]_2$
15	318.77	256	He*I*	19.81	23.70	$1s2s\ ^3S_1$	$1s4p\ ^3P_2$
16	328.06	2793	Ag*I*	0.00	3.77	$4d^{10}5s\ ^2S_{1/2}$	$4d^{10}5p\ ^2P_{3/2}$
17	338.28	2589	Ag*I*	0.00	3.66	$4d^{10}5s\ ^2S_{1/2}$	$4d^{10}5p\ ^2P_{1/2}$
18	388.86	1129	He*I*	7.42	23.00	$1s2s\ ^3S_1$	$1s3p\ ^3P_1$
19	405.54	356	Ag*I*	3.66	6.72	$4d^{10}5p\ ^2P_{1/2}$	$4d^{10}6d\ ^2D_{3/2}$
20	421.09	417	Ag*I*	3.77	6.72	$4d^{10}5p\ ^2P_{3/2}$	$4d^{10}6d\ ^2D_{5/2}$
21	447.14	905	He*I*	20.96	23.73	$1s2p\ ^3P_1$	$1s4d\ ^3D_2$
22	487.41	465	Ag*I*	7.30	9.84	$4d^95s(^3D)5p\ ^4F_{9/2}$	$4d^95s(3D)6s\ ^4D_{7/2}$
23	490.24	508	S*II*	15.55	18.08	$3s^23p^2(^3P)4p\ ^2S_{1/2}$	$3s3p^4\ ^2P_{1/2}$
24	501.56	673	He*I*	20.61	23.08	$1s2s\ ^1S_0$	$1s3p\ ^1P_1$
25	520.90	2482	Ag*I*	3.66	6.04	$4d^{10}5p\ ^2P_{1/2}$	$4d^{10}5d\ ^2D_{3/2}$
26	546.54	3888	Ag*I*	3.77	6.04	$4d^{10}5p\ ^2P_{3/2}$	$4d^{10}5d\ ^2D_{5/2}$
27	587.59	11174	He*I*	20.96	23.07	$1s2p\ ^3P_2$	$1s3d\ ^3D_2$
28	657.07 –328.06(2)	5157	Ag*I*	0.00	3.77	$4d^{10}5s\ ^2S_{1/2}$	$4d^{10}5p\ ^2P_{3/2}$
29	667.81	2663	He*I*	21.21	23.07	$1s2p\ ^1P_1$	$1s3d\ ^1D_2$
30	679.2 –338.28(2)	2253	Ag*I*	0.00	3.66	$4d^{10}5s\ ^2S_{1/2}$	$4d^{10}5p\ ^2P_{1/2}$
31	706.51	1498	He*I*	20.96	22.71	$1s2p \rightarrow {}^3P_2$	$1s3s\ ^3S_1$
32	777.19	1669	O*I*	9.14	10.74	$3s\ ^5S^0_2$	$3p\ ^5P_3$

The most intense lines were the resonant spectral lines of the silver atom at 328.06 nm of Ag*I* and 338.28 nm of Ag*I*. The 224.64 lines stood out from the ion spectral lines by intensity at 232.02 nm.

The most intense spectral lines include lines 388.86, 447.14, 501.56, 587.59, 667.81, 706.51 nm of He*I*. These lines of the He atom in a pulsed atmospheric pressure plasma are observed, when the process of energy transfer from the lower metastable levels of He*I* to some impurity (for example, silver sulphide molecules and its dissociation products) is effective [11, 12].

When the frequency of voltage pulses was reduced to 80 Hz and the He pressure was reduced to 13.3 kPa, a decrease in the intensity of all spectral lines of silver was observed that is caused by a decrease in the concentration of the electrode material in the discharge plasma.

The formation of excited silver atoms and ions can occur during the excitation of a silver atom by electrons, in the processes of excitation of a singly charged silver ion by electrons with subsequent recombination of silver ions (Ag*II*, Ag*III*).

When the quartz substrate was installed at a distance of 2–3 cm from the centre of the discharge gap and the burning time of the discharge was of 30–60 minutes, the deposition of a thin film from the products of sputtering of the electrode material in atmospheric-pressure helium was recorded on the substrate (Fig. 5). As can be seen from this photo, the surface of the synthesized thin film is quite uniform. Against the background of a homogeneous surface, individual surface microstructures with characteristic dimensions of

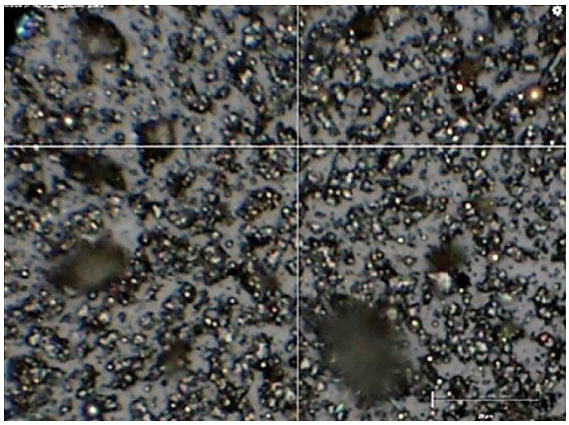

Fig. 5. Photo of the surface of the current film obtained at a 50-fold magnification and synthesized from OND products between electrodes from the superionic conductor Ag_2S at atmospheric pressure of helium.

10–20 μm can be observed (in the photo, they have a dark gray colour and an ellipsoidal shape). It is most likely that these are pieces broken off from the electrodes, when their surface is affected by the powerful electric field of the OND. Therefore, in order to improve the uniformity of the film, it is worth reducing the pulsed power of the OND energy contribution to the plasma.

Of all buffer inert gases (Ne, Ar, Kr), the energy characteristics of OND in Ne are minimal. It is also possible to reduce the energy characteristics of the OND by reducing the pressure of the buffer gas and the magnitude of the electric field between the electrodes (lowering the charging voltage on the anode of the thyratron), but this will lead to significant changes in the value of the E/N parameter, as indicated by the results of modelling plasma parameters [2] and the result of calculations shown below.

Figures 6–8 show the Raman spectra of a thin film that was synthesized from OND products between silver sulphide electrodes at atmospheric helium pressure using laser radiation at wavelengths $\lambda = 785$ nm, $\lambda = 532$ nm and $\lambda = 633$ nm, in accordance. The use of different wavelengths of laser radiation allows obtaining additional information about the properties of Ag_2S nanoparticles, since the intensity and position of the bands in the Raman scattering spectra depend on the wavelength of the excitation radiation. The wavelength affects the depth of radiation penetration into the sample and the efficiency of the induced oscillations in the crystals. This can lead to a difference in the intensity and position of the spectral bands of scattered light.

When examining the samples using laser radiation at $\lambda = 785$ nm, the spectra in Fig. 6, *a*, *b*, *c* are characterized by bands in the range of 100–300 cm^{-1}, in particular, at 228 cm^{-1} (Fig. 6, *a*), 235 cm^{-1} (Fig. 6, *c*); laser spectrum at $\lambda = 532$ nm in Fig. 7, *a* are characterized by bands in the range of 100–300 cm^{-1}, in particular, at 242 cm^{-1} (Fig. 7, *a*); laser spectra at $\lambda = 633$ nm are characterized by bands in the range of 100–300 cm^{-1}, in particular, at 238 cm^{-1} (Fig. 8, *a*), 242 cm^{-1} (Fig. 8, *b*). Broad bands in the range of 210–250 cm^{-1}, in particular, the maxima in this range given above caused by Ag_2S nanoparticles, are associated with symmetric longitudinal vibrational modes of Ag–S–Ag bonds. Bands with a maximum at 604 cm^{-1} (Fig. 6, *c*), 595 cm^{-1} (Fig. 8, *a*), 602 cm^{-1} (Fig. 8, *b*) can be attributed to O–S–O bonds (asymmetric bending). Bands with a maximum at 960 cm^{-1} (Fig. 2, *c*), 957 cm^{-1} (Fig. 8, *a*–*d*) refer to the symmetric stretching of S–O bonds.

In Figures 6, *b*, 7, *b*, 8, *d*, visible broad bands in the range of 1460–1600 cm^{-1} are associated with fluctuations of silver and sulphur oxide compounds, which are formed during the photoinduced decomposition of Ag_2S.

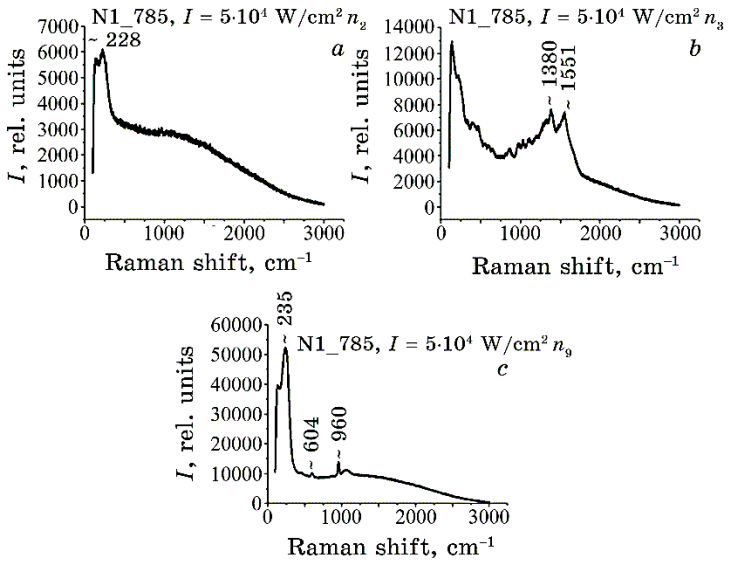

Fig. 6. Raman spectra of light scattering by a thin film deposited from OND plasma at atmospheric helium pressure, which were obtained using laser radiation at $\lambda = 785$ nm (*a*, *b*, *c*).

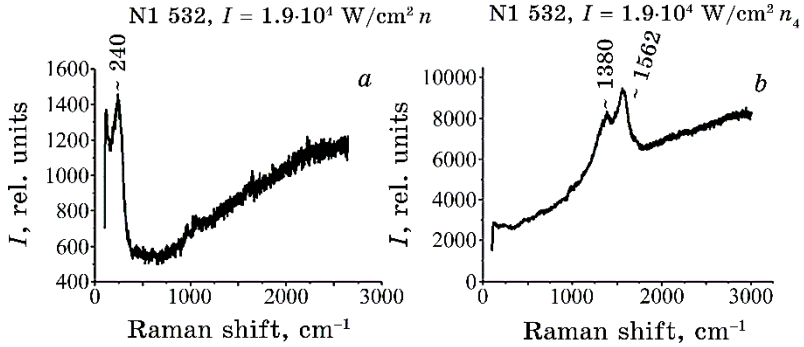

Fig. 7. Raman spectra of light scattering by a thin film deposited from an OND plasma at atmospheric helium pressure, which were obtained using laser radiation at $\lambda = 532$ nm (*a*, *b*).

Therefore, the results showed that the Raman spectra reflect the characteristic features of Ag_2S films and their oxides. In particular, bands were observed that corresponded to chemical bonds in the composition of Ag_2S compounds. This indicates a successful synthesis and formation of films with the desired properties.

Let us consider the results of numerical modelling of the parameters of the OND plasma in the He–Ag_2S gas–vapour mixture.

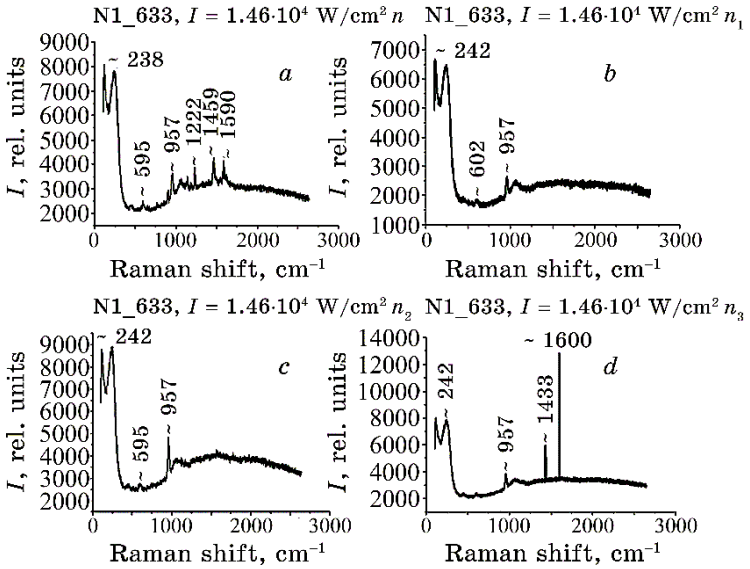

Fig. 8. Raman spectra of light scattering by a thin film deposited from OND plasma at atmospheric helium pressure, which were obtained using laser radiation at $\lambda = 633$ nm (*a*–*d*).

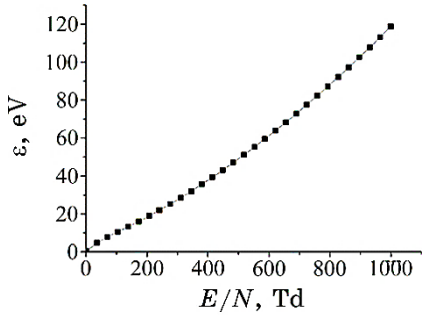

Fig. 9. Dependence of the average energy of electrons in the plasma of a gas–vapour mixture, He:Ag_2S = 101000:300 [Pa], at a total pressure p = 101300 Pa on the value of the parameter E/N.

Figure 9 shows the dependence of the average energy of electrons in the discharge on the value of the reduced electric field strength for the gas–vapour mixture He:Ag_2S = 101000:300 [Pa].

The mean energy of discharge electrons in the gas–vapour mixture increased from 0.3778 to 118.8 eV (Fig. 9) as the reduced electric-field strength increased from 1 to 1000 Td. At the same time, an increase in the rate of its change was observed in the range of growth of the E/N parameter from 100 to 1000 Td.

TABLE 3. Electron-transport characteristics for times 60 and 180 ns at electric-field strength $E = 8 \cdot 10^6$ V/m and $1.3 \cdot 10^6$ V/m for a discharge in a gas–vapour mixture $He:Ag_2S = 101000:300$ [Pa] at total pressure $p = 101300$ Pa.

τ, ns	E/N, Td	Mixture $He:Ag_2S = 101000:300$ [Pa]			
		ε, eV	T, K	V_{dr}, m/s	N_e, m^{-3}
60	327	28. 54	331 064	$6.7 \cdot 10^5$	$2.4 \cdot 10^{19}$
180	53	4.774	51 898	$8.4 \cdot 10^4$	$2.3 \cdot 10^{20}$

TABLE 4. The value of the specific power of discharge losses due to the elastic and inelastic processes of collisions of electrons with helium and silver atoms in the plasma of the steam–gas mixture $He:Ag_2S = 101000:300$ [Pa] for the reduced electric-field strength on the plasma, which was reached at the moment of time τ = 60 ns and 130 ns from the start of the breakdown of the bit gap.

Mixture $He:Ag_2S = 101000:300$ [Pa]		
E/N, Td	Elastic, Power/N, eV·m^3/s	Inelastic, Power /N, eV·m^3/s
327	$0.4371 \cdot 10^{-15}$	$0.1519 \cdot 10^{-12}$
53	$0.1041 \cdot 10^{-15}$	$0.2532 \cdot 10^{-14}$

Table 3 shows the results of calculating the transport characteristics of discharge electrons: mean energy (ε), temperature (T, K) and drift speed ($V_{dr.}$) of electrons for plasma on a mixture of helium and silver. The following regularities were observed: the mean energy, temperature, and electron drift speed increased with an increase in the applied voltage and were of 28.54 eV and 4.774 eV, 331.064 K and 51.898 K, $6.7 \cdot 10^5$ m/s and $8.4 \cdot 10^4$ m/s for $E/N = 327$ Td and 53 Td, respectively, which were reached at the time τ = 60 ns and 180 ns from the start of breakdown between the electrodes. The values of the electron concentration at these moments of time were of $2.4 \cdot 10^{19}$ m^{-3} and $2.3 \cdot 10^{20}$ m^{-3} at the current density of (2.55 and 3.06)$\cdot 10^6$ A/m^2 on the surface of the electrode of the radiation source ($0.196 \cdot 10^{-4}$ m^2) for the reduced electric-field strengths $E/N = 327$ Td and 53 Td (Fig. 2).

Table 4 shows the values of the specific power of discharge losses due to elastic and inelastic processes of collisions of electrons with helium and silver atoms in the plasma of the gas–vapour mixture $He:Ag_2S = 101000:300$ [Pa] at a total pressure of $p = 101300$ Pa for the reduced electric-field strength between the electrodes, which was reached at the time τ = 60 ns and 180 ns from the start of breakdown. The maximum value of the specific power of discharge losses was obtained for inelastic processes, and it was of $0.1519 \cdot 10^{-12}$

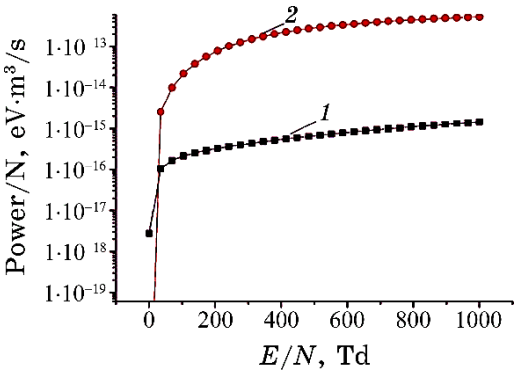

Fig. 10. Dependence of the specific power of discharge losses on the elastic and inelastic processes of collisions of electrons with helium and silver atoms on the reduced electric-field strength in the plasma of the vapour–gas mixture $He:Ag_2S = 101000:300$ [Pa] at a total pressure of $p = 101300$ Pa.

eV·m^3/s for $E/N = 327$ Td.

Specific discharge power losses in the mixture of $He:Ag_2S = 101000:300$ [Pa] were the largest for elastic scattering on helium atoms (Fig. 10, curve *1*) at $E/N = 1$ Td. For the total inelastic scattering and ionization of electrons on silver atoms, they were of 80% for $E/N = 35.4$ Td; a smaller value (34.8%) was reached for $E/N = 248$ Td for the process of atom ionization helium. Excitation of the energy level of helium atoms (threshold energy of 19.80 eV), namely, by 27.3% at $E/N = 104$ Td, and for ionization of silver atoms, by 5% at $E/N = 50$ Td. The specific discharge power losses for the excitation of energy levels of silver atoms had maximum values at $E/N = 30$ Td for the excitation of energy levels of silver atoms (threshold energy of 3.78 eV, $\lambda = 328.068$ nm and threshold energy of 3.66 eV, $\lambda = 338.289$ nm), and they are of 3.8% and 2.2%, respectively.

This completeness was consistent with the radiation spectrum of the discharge, where these spectral lines were the most intense (Fig. 2), for ionization of silver atoms (threshold energy of 8 eV), by 3.2% at a reduced electric-field strength of 70 Td.

The rate of rise and fall of discharge power losses due to the processes of excitation of electronic states and ionization and its magnitude are related to the nature of the dependence of the effective cross sections of inelastic processes of collisions of electrons with the components of the mixture on the energies of electrons, their absolute values, and the dependence of the electrons' distribution function on the values of the reduced field strength and threshold energy values of the process.

The rate constants of electron collisions with helium and silver at-

TABLE 5. Excitation-rate constants of the spectral lines of silver atoms for fixed values of the reduced electric-field strength in the plasma on a gas–vapour mixture of helium with silver at time points of 50 ns and 100 ns from the start of discharge ignition.

E/N, Td	Mixture He:Ag = 101000:300 [Pa]					
327	Ag	λ, nm	328.06	338.28	405.54	421.09
		k, m^3/s	$0.1914 \cdot 10^{-12}$	$0.1138 \cdot 10^{-12}$	$0.2362 \cdot 10^{-15}$	$0.2362 \cdot 10^{-15}$
53	Ag	λ, nm	328.068	338.289	405.54	421.09
		k, m^3/s	$0.9089 \cdot 10^{-14}$	$0.5541 \cdot 10^{-17}$	$0.5791 \cdot 10^{-17}$	$0.5791 \cdot 10^{-17}$

oms on the E/N parameter in the discharge on gas–vapour mixtures varied in the range of $k \approx 10^{-12}$–10^{-29} m^3/s that is related to the values of the absolute effective cross sections of the corresponding processes. For silver atoms, they are maximal for the excitation of lines with wavelengths λ = 328.06 nm and 338.28 nm (Table 5) and reached values of $0.1914 \cdot 10^{-12}$ m^3/s and $0.1138 \cdot 10^{-12}$ m^3/s at the value of the reduced electric field of 327 Td. The elastic-scattering rate constant of electrons on helium atoms was greater than the elastic-scattering rate constant on silver atoms, namely, $0.6666 \cdot 10^{-13}$ on helium and $0.1815 \cdot 10^{-12}$ on silver, both for the parameter $E/N = 327$ Td, and for the parameter $E/N = 53$ Td of the reduced electric field, they are of $0.7151 \cdot 10^{-13}$ on helium and $0.4276 \cdot 10^{-13}$ on silver.

4. CONCLUSIONS

As a result of studies of the characteristics and parameters of the plasma of an overvoltage nanosecond discharge in helium at atmospheric pressure between electrodes made of a polycrystalline Ag_2S compound, the following was revealed:

— with the total duration of the voltage pulses up to 450 ns, the maximum amplitude of the voltage of positive polarity between the electrodes reached 17 kV, and the maximum amplitude of the current pulses reached 150 A, the largest pulsed electric power of the discharge reached 2.3 MW with the energy in a single pulse of 91 mJ; decreasing the helium pressure to 13.3 kPa led to a decrease in the amplitudes of voltage, current, and pulse power, and the energy in the pulse decreased to 35.6 mJ, the maximum intensity of UV radiation was achieved at the atmospheric pressure of helium, the frequency was of 1000 Hz, and the value of the charging voltage was of 19 kV;

— discharge plasma radiated in the UV range of wavelengths at the transitions of an atom and a singly charged silver ion; resonance spectral lines of the silver atom (328.06 and 338.28 nm of Ag*I*)

were distinguished by intensity; the discharge plasma is the source of the flow of UV radiation and the flow of silver sulphide nanostructures that is promising for applications in micro-nanotechnology, microbiology and biomedical engineering; the highest intensity of UV radiation at the transitions of atoms and singly charged silver ions was obtained at the atmospheric pressure of helium at the repetition frequency of voltage pulses $f = 1000$ Hz;
— surface microstructures with dimensions of 10–20 μm were synthesized during deposition of electrode-erosion products on a quartz substrate installed near the electrode system;
— the results of Raman light-scattering spectra of synthesized films showed that they consist exclusively of silver sulphide and are quite homogeneous in terms of surface structure;

Analysis of the plasma parameters of an overvoltage discharge in a gas–vapour mixture of helium and silver sulphide showed the following patterns:
— an increase in the reduced electric-field intensity led to an increase in the number of 'fast' electrons in the discharge and an increase in the mean electron energy from 0.3778 eV to 118.8 eV in the range of $E/N = 1$–1000 Td; the mean energy, temperature, and electron drift speed increased with increasing applied voltage and were of 4.774 eV and 28.54 eV, 51898 K and 331064 K, $8.4 \cdot 10^4$ m/s and $6.7 \cdot 10^5$ m/s for $E/N = 53$ Td and 327 Td, respectively, which were reached at the moment of time $\tau = 180$ ns and 60 ns from the beginning of the breakdown between the electrodes; the electron concentration at these moments was of $2.3 \cdot 10^{20}$ m^{-3} and $2.4 \cdot 10^{19}$ m^{-3} for reduced electric-field strength $E/N = 53$ Td and 327 Td;
— an increase in power losses was observed with an increase in the reduced electric-field strength, both for elastic electronic processes and for inelastic electronic processes; for inelastic processes, discharge losses were approximately three orders of magnitude higher for $E/N = 327$ Td and approximately two orders of magnitude higher for $E/N = 53$ Td; the maximum value of the specific power of discharge losses was for inelastic processes, and it was equal to $0.1519 \cdot 10^{-12}$ eV·m^3/s for $E/N = 327$ Td; the specific discharge power losses for the excitation of the energy levels of silver atoms had maximum values at $E/N = 30$ Td for the excitation of the energy levels of silver atoms at $\lambda = 328.068$ nm and $\lambda = 338.289$ nm, and they are of 3.8% and 2.2%, respectively; for ionization of silver atoms, λ loss is of 3.2% at $E/N = 70$ Td.

Taking into account the results of our work [20], in which the characteristics of OND between selenium electrodes in an inert gas atmosphere are given, it is possible to propose a gas-discharge plasma chemical reactor based on OND for the synthesis of complex compounds of the Ag_2Se–Ag_2S type, which will combine the proper-

ties of individual silver chalcogens and can find new fields of application in medicine, biomedical engineering and biotechnology. For this, one electrode made of selenium and another one made of sulphur sulphide should be installed in the reactor and filled with helium at atmospheric pressure.

REFERENCES

1. Alexander Shuiabov, Alexander Minya, Antonina Malinina, Alexander Malinin, Roman Golomb, Igor Shevera, Zoltan Gomoki, and Vladislav Danilo, *Advances in Natural Sciences: Nanoscience and Nanotechnology*, **9**, No. 3: 035018 (2018); https://doi.org/10.1088/2043-6254/aadc4b
2. O. K. Shuaibov, O. Y. Mynia, A. O. Malinina, R. V. Hrytsak, and O. M. Malinin, *Ukrainian Journal of Physics*, **67**, No.4: 240 (2022) (in Ukrainian); https://doi.org/10.15407/ujpe67.4.240
3. O. K. Shuaibov, O. Y. Minya, A. O. Malinina, O. M. Malinin, and I. V. Shevera, *Nanosistemi, Nanomateriali, Nanotehnologii*, **19**, Iss. 1: 189 (2021); https://doi.org/10.15407/nnn.19.01.189
4. O. K. Shuaibov and A. O. Malinina, *Progress in Physics of Metals*, **22**, No. 3: 382 (2021); https://doi.org/10.15407/ufm.22.03.382
5. G. A. Mesyats, *Usp. Fizich. Nauk*, **165**, No. 6: 601 (1995); https://doi.org/10.1070/%20PU1995v038n06ABEH000089
6. V. F. Tarasenko, *Runaway Electrons Preionized Diffuse Discharge* (New York: Nova Science Publishers Inc.: 2014).
7. A. K. Abduev, A. S. Asvarov, A. K. Akhmedov, R. M. Emiro, and V. V. Belyaev, *Tech. Phys. Lett.*, **43**: 1016 (2017); https://doi.org/10.1134/S1063785017110153
8. Zh. Liu, A. A. Rogachev, M. A. Yarmoolenko, H. N. Zhang, A. V. Rogachev, and D. L. Gorbachev, *Problems of Physics, Mathematics and Technology*, **4**, No. 1: 13 (2013).
9. S. I. Sadovnikov, A. A. Rempel', and A. I. Gusev, *JETP Lett.*, **106**: 587 (2017); https://doi.org/10.1134/S002136401721010X
10. *NIST Atomic Spectra Database Lines Form*; https://physics.nist.gov/PhysRefData/ASD/lines_form.html
11. A. K. Shuaibov, *Czechoslovak Journal of Physics*, **49**, No. 2: 225 (1999); https://doi.org/10.1023/A:1022806112782
12. O. K. Shuaibov, *Multielectrode Corona Discharge in High-Pressure Gases* (Uzhgorod: Publishing House of Uzhgorod National University 'Hoverla': 2015) (in Ukrainian).
13. G. J. M. Hagelaar and L. C. Pitchford, *Plasma Sources Sci. Techn.*, **14**, No. 4: 722 (2005); https://doi.org/10.1088/0963-0252/14/4/011
14. *BOLSIG+, Electron Boltzmann Equation Solver* [Electronic resource]; Resource access mode: http://www.bolsig.laplace.univ-tlse.fr/
15. Yu. M. Smirnov, *Journal of Technical Physics*, **69**, No. 2: 6 (1999).
16. D. Gupta, R. Naghma, and B. Antony, *Can. J. Phys.*, **91**: 744 (2013); https://doi.org/10.1139/cjp-2013-0174,%20P%20744-750
17. Yu. M. Smirnov, *Quantum Electronics*, **29**, No. 2: 168 (1999); https://doi.org/10.1070/qe1999v029n01ABEH001381

18. O. K. Shuaibov, R. V. Hrytsak, O. I. Minya, Z. T. Gomoki, and M. I. Vatrala, *Metallofiz. Noveishie Tekhnol.*, **44**, No. 11: 1509 (2022) (in Ukrainian); https://doi.org/10.15407/mfint.44.11.1509
19. I. Martina, R. Wiesinger, and M. Schreiner, *J. Raman Spectrosc.*, **44**, No. 5: 770 (2013); https://doi.org/10.1002/jrs.4276
20. Oleksandr Shuaibov, Oleksandr Minya, Roksolana Hrytsak, Antonina Malinina, Oleksandr Malinin, Yuriy Bilak, and Zoltan Homoki, *Journal of Clinical and Biomedical Advances*, **3**, No. 1: 1 (2024); doi:10.63620/MKJCBA.2024.1018